The primary defect in experimental ileitis originates from a nonhematopoietic source

Timothy S. Olson,[1,3] Brian K. Reuter,[2] Kevin G-E. Scott,[2] Margaret A. Morris,[3,4] Xiao-Ming Wang,[2] Leslie N. Hancock,[2] Tracy L. Burcin,[3,4] Steven M. Cohn,[2] Peter B. Ernst,[2] Fabio Cominelli,[2] Jonathan B. Meddings,[5] Klaus Ley,[3,4] and Theresa T. Pizarro[2]

[1]Department of Molecular Physiology, [2]Digestive Health Center of Excellence, [3]Robert M. Berne Cardiovascular Research Center, and [4]Department of Biomedical Engineering, University of Virginia Health System, Charlottesville, VA 22908
[5]Department of Medicine, University of Alberta, Edmonton, AB, Canada T6G 2B7

The initiating etiologic factor in Crohn's disease (CD) remains unclear. SAMP1/YitFc (SAMP) mice develop chronic ileitis similar to human CD. We used bone marrow chimeras to determine if SAMP ileitis results from a primary immunological defect or from dysregulated mucosal immunity secondary to intrinsic, nonhematopoietic (e.g., epithelial) dysfunction. SAMP mice receiving wild-type (AKR) BM developed severe ileitis, whereas SAMP BM did not confer ileitis to WT recipients. WT lymphocytes from reconstituted SAMP mice resembled native SAMP populations in regard to surface phenotype and cytokine production. Ilea from native SAMP mice and SAMP recipients of wild-type BM displayed decreased epithelial barrier resistance ex vivo and increased epithelial permeability in vivo compared to native WT mice and AKR recipients of SAMP BM. This permeability defect preceded the development of ileal inflammation, was present in the absence of commensal bacteria, and was accompanied by altered ileal mRNA expression of the tight junction proteins claudin-2 and occludin. Our results provide evidence that the primary defect conferring ileitis in SAMP mice originates from a nonhematopoietic source. Generation of pathogenic lymphocytes is a consequence of this defect and does not reflect intrinsic proinflammatory leukocyte properties. Decreased barrier function suggests that defects in the epithelium may represent the primary source of SAMP ileitis susceptibility.

CORRESPONDENCE
Theresa T. Pizarro:
ttp4e@virginia.edu

Abbreviations used: BMT, bone marrow transplant; CD, Crohn's disease; CLDN, claudin; FE, fractional excretion; GF, germ-free; HGPRT, hypoxanthine-guanine phosphoribosyl transferase; MLN, mesenteric lymph node; MPO, myeloperoxidase; SAMP, SAMP1/YitFc; SPF, specific pathogen-free; TEER, transepithelial electrical resistance; TJ, tight junction.

Many considerable advances have recently been made in the field of Crohn's disease (CD) research, enabling both a better understanding of the mucosal immune system (1) and the advent of more effective treatment modalities (2). However, the primary defect in genetically susceptible individuals that initiates the cascade of events leading to the development of disease remains largely unknown (3, 4). One of the key unresolved issues regarding this susceptibility trait, underscored by the fact that recently discovered susceptibility genes are expressed and possess independent functions in both hematopoietic cells and intestinal epithelial cells (5, 6), concerns the cells or tissue in which this precipitating factor originates.

Many lines of evidence suggest that a primary immunologic defect may be responsible for the development of CD (1). Aberrant lamina propria mononuclear cell overexpression of T helper (Th)1 polarizing cytokines, such as IL-12 and IFNγ, has long been postulated as a potential causal factor of CD (7, 8). In murine adoptive transfer models, $CD45RB^{hi}$ or $CD25^{-}$ $CD4^{+}$ T cell populations expressing these cytokines are sufficient to induce colitis with pathologic features resembling CD colitis (9, 10). Primary defects in the function of regulatory T cells, which can block colitis in animal models through TGFβ- and IL-10–dependant mechanisms (11), may give rise to intestinal inflammation by allowing excessive effector responses to nonpathogenic floral or food antigens (12, 13). Increased serum autoreactivity in CD patients and the proinflammatory effect of B cells in models of ileitis suggest that B lymphocyte specificity may be involved in initiating the disease (14, 15), whereas the curative effect of enhancing myeloid cell function

T.S. Olson and B.K. Reuter contributed equally to this work.

in a cohort of CD patients (16) suggests that defects in myeloid cells may also play a critical role. Most convincingly, case reports have demonstrated complete remission in several CD patients after irradiation and allogeneic BM transplantation (17), suggesting a primary defect in immune cell function in these individuals.

Conversely, there are several lines of evidence suggesting that intestinal epithelial cells confer the primary susceptibility to CD. Paneth cell-derived NOD2 from normal individuals may play a critical role in the ability of epithelial cells to expel luminal bacteria, whereas CD-variant NOD2 lacks this function (6). Epithelial toll-like receptor expression is altered in CD patients (18), suggesting that the inability of the epithelium to respond properly to common bacterial motifs might lead to disease initiation. Epithelial cytokine and chemokine expression is also increased in the context of CD (19, 20), possibly enabling the initial recruitment of inflammatory cells to lesion sites. Importantly, alterations in epithelial barrier function have been proposed to be a primary etiologic factor leading to CD, as intestinal permeability is dramatically increased in CD patients relative to normal controls or ulcerative colitis patients (3, 21). In fact, first degree relatives of CD patients who are at increased risk for developing the disease often have increased intestinal permeability relative to the general population (22, 23). Furthermore, increased epithelial permeability often precedes and predicts relapse after remission for CD patients (24). Collectively, these findings suggest that dysregulated barrier function may be a prerequisite for the onset of intestinal inflammation such as that observed in CD (21).

Epithelial permeability is primarily controlled at the level of tight junctions (TJs). The density of TJ strands determines tissue-specific size restrictions on passage through tight junctional pores (25), with estimates suggesting that particles bigger than 2,000 D are typically excluded by intestinal epithelial TJs (26). The two major structural constituents of TJs are heterohexamers of claudins (isoforms 1–5), which form the actual pore, and the adjacent occludin molecules, both of which form homotypic interactions with counterparts on neighboring cells (27). Interactions between distinct claudin isoforms possess different affinities such that regulation of isoform-specific expression patterns may provide one method of permeability regulation (28, 29). Only one isoform of occludin is known, and its regulation occurs primarily through relocalization of the protein by dephosphorylation (30). The large protein zonula occludens (ZO)-1 serves as a scaffolding protein, linking claudins and occludins with the actinomyosin ring of the epithelial cell. Many cellular signals aimed at altering permeability affect the expression or junctional localization of ZO-1 (31).

The SAMP1/YitFc (SAMP) murine model of chronic intestinal inflammation provides an excellent system in which to study the contributions made by specific tissues and cell types to the development of CD, partly because it is one of the few models in which inflammation is most severe in the terminal ileum, the hallmark location of CD lesions (32, 33). Additionally, because this mouse strain was derived from brother-sister breeding of WT AKR mice (34), the phenotype occurs spontaneously as in the human condition, without chemical, genetic, or immunologic manipulation. The inflammatory lesions develop by 10 wk of age (35) and mostly consist of Th1-type immune responses (36), although Th2-polarizing cytokines also contribute to disease pathogenesis (37). Mesenteric lymph node (MLN) $CD4^+$ T cells, capable of adoptively transferring the ileitis phenotype to SCID mice, and aberrantly expanded MLN and lamina propria B cell populations help drive the SAMP ileal inflammatory response (36, 38), and the severity of disease can be decreased by either antibiotics or anti-TNF antibodies (39, 40). Genetic outcross studies and linkage analysis have identified loci on several SAMP chromosomes with polymorphic markers that segregate with the ileitis phenotype, including polymorphisms in the promoter region of the peroxisome proliferator-activated receptor-γ (Pparγ) gene that affect expression in an epithelial cell–specific fashion (41,42).

In the present study, we investigated whether the primary etiologic factor responsible for SAMP ileitis originates from immune cells or a nonhematopoietic source, such as the intestinal epithelium. Construction of chimeric mice was achieved using BM transplantation in which AKR and SAMP mice were reconstituted with SAMP and AKR BM, respectively, and assayed for the severity of gut inflammation. We next examined the effect of exchanging hematopoietic cell compartments on the size of lymphocyte subsets and T cell cytokine production within recipient mice. Epithelial barrier function was then evaluated in both native SAMP and AKR mice as well as in bone marrow transplant (BMT) recipients. We then performed a time-course study, comparing the onset of the permeability defect in SAMP ileum versus the development of ileal inflammation and neutrophil infiltration in both conventionally housed and germ-free (GF) SAMP mice. Finally, we examined the expression of TJ proteins in young SAMP versus AKR ileum, before the onset of inflammation, to determine whether differential regulation of these proteins may lead to the permeability defect. Collectively, our data demonstrate that a nonhematopoietic tissue, likely the intestinal epithelium, contains the primary ileitis susceptibility factor in SAMP mice, and this factor, which may involve aberrant TJ formation leading to increased paracellular permeability through the epithelial barrier, is capable of educating normal WT leukocytes to become pathogenic and promote the development of CD-like ileitis.

RESULTS

BMT between SAMP and AKR mice results in full leukocyte reconstitution

To test relative contributions of the epithelium and leukocytes to the primary ileitis susceptibility in SAMP mice, we generated BM chimeras by reconstituting irradiated SAMP mice with WT AKR BM (AKR BM → SAMP) and irradiated AKR mice with SAMP BM (SAMP BM → AKR). We tested the amount of hematopoietic cell reconstitution

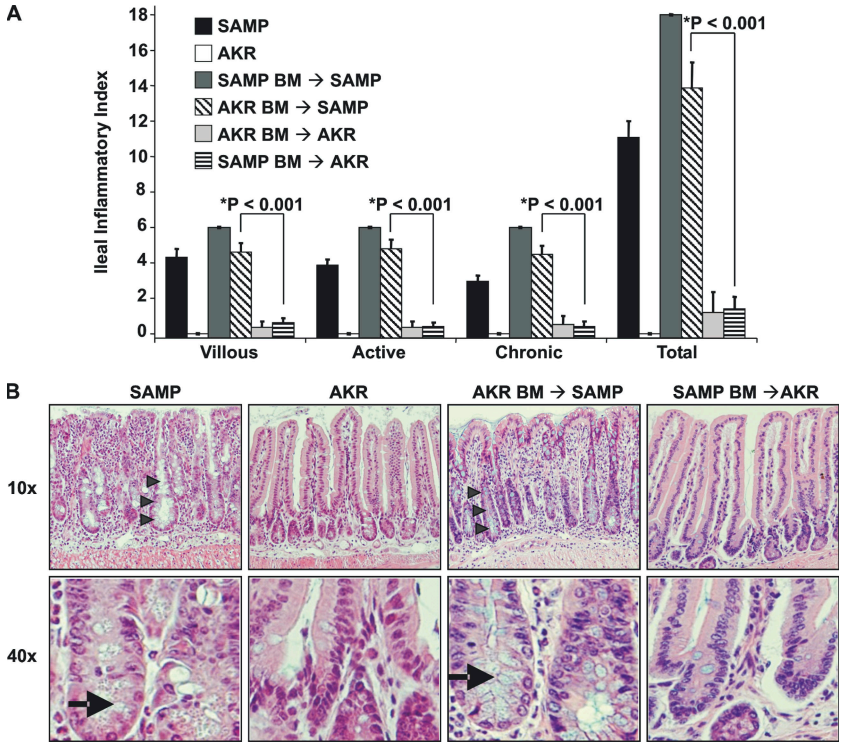

Figure 1. Ileitis is dependent on host/nonhematopoietic compartment and not donor BM. (A) Disease severity was assessed in SAMP ($n = 7$), AKR ($n = 5$), SAMP BM → SAMP ($n = 5$), AKR BM → SAMP ($n = 10$), AKR BM → AKR ($n = 3$), and SAMP BM → AKR ($n = 10$) mice. *Significant difference in inflammatory score between SAMP BM → AKR and AKR BM → SAMP mice. (B) Histologic evaluation of ileal sections from SAMP and AKR BM → SAMP mice shows large inflammatory infiltrates and epithelial abnormalities including crypt hypertrophy and elongation (arrowheads), and Paneth cell hyperplasia (arrows). Sections from AKR and SAMP BM → AKR mice display normal architecture.

by transplanting female recipients with male BM cells and assaying for the amount of Y chromosome DNA within leukocyte compartments 6 wk after irradiation and transplantation using quantitative real-time PCR. By comparing with a standard curve of known ratios of male to female DNA, we determined that reconstitution was ≥94% for AKR BM → SAMP and SAMP BM → AKR splenocytes. The percentage of reconstitution was >80% in all tissues assayed, with a trend toward slightly higher reconstitution in SAMP BM → AKR mice versus AKR BM → SAMP mice.

Ileitis phenotype tracks with SAMP host/epithelium, not SAMP BM

We next assessed inflammation severity in reciprocal BMT mice 6 wk after transplant using an established histologic scoring system (43). AKR BM → SAMP mice exhibited a trend toward slightly higher levels of overall inflammation (total inflammatory index, 14 ± 1, mean ± SEM) compared with native SAMP mice (11 ± 1) (Fig. 1 A). The transplantation procedure itself may increase the severity of SAMP ileitis, as SAMP BM → SAMP possessed significantly higher ileal inflammatory scores (18 ± 0) compared with native SAMP mice. However, SAMP BM → SAMP ileitis was not significantly more severe than AKR BM → SAMP ileitis. Furthermore, the inflammatory scores in AKR BM → SAMP ilea for all three individual histologic indices, including epithelial architectural destruction as well as active and chronic inflammation, were comparable to scores for native SAMP mice. In contrast, SAMP BM → AKR mice developed only mild, if any, inflammation (1.4 ± 0.7), comparable to levels seen in irradiated AKR mice reconstituted with AKR BM (1.2 ± 1.2), suggesting that the primary susceptibility leading to ileitis in SAMP mice originates from a nonhematopoietic source. Ileal inflammatory scores from either AKR BM → SAMP or SAMP BM → AKR mice at 12 wk after transplant followed the same pattern, with AKR BM → SAMP mice exhibiting severe ileitis and SAMP BM → AKR mice developing only mild inflammation (unpublished data). Scores at 12 wk after transplant were not significantly different from the respective scores in the same group of mice at 6 wk after transplant.

The ileitis in AKR BM → SAMP mice was histopathologically similar to that observed in native SAMP mice (Fig. 1 B). Both AKR BM → SAMP and native SAMP ileum displayed thickening of the muscularis layer and dense inflammatory infiltrates composed of both acute and chronic inflammatory cells throughout the villi and within the submucosa. Additionally, several epithelial abnormalities observed in SAMP mice were also noted in AKR BM → SAMP mice, including villous blunting, crypt hypertrophy and elongation, and abnormal hypertrophy and hyperplasia of Paneth and goblet cells.

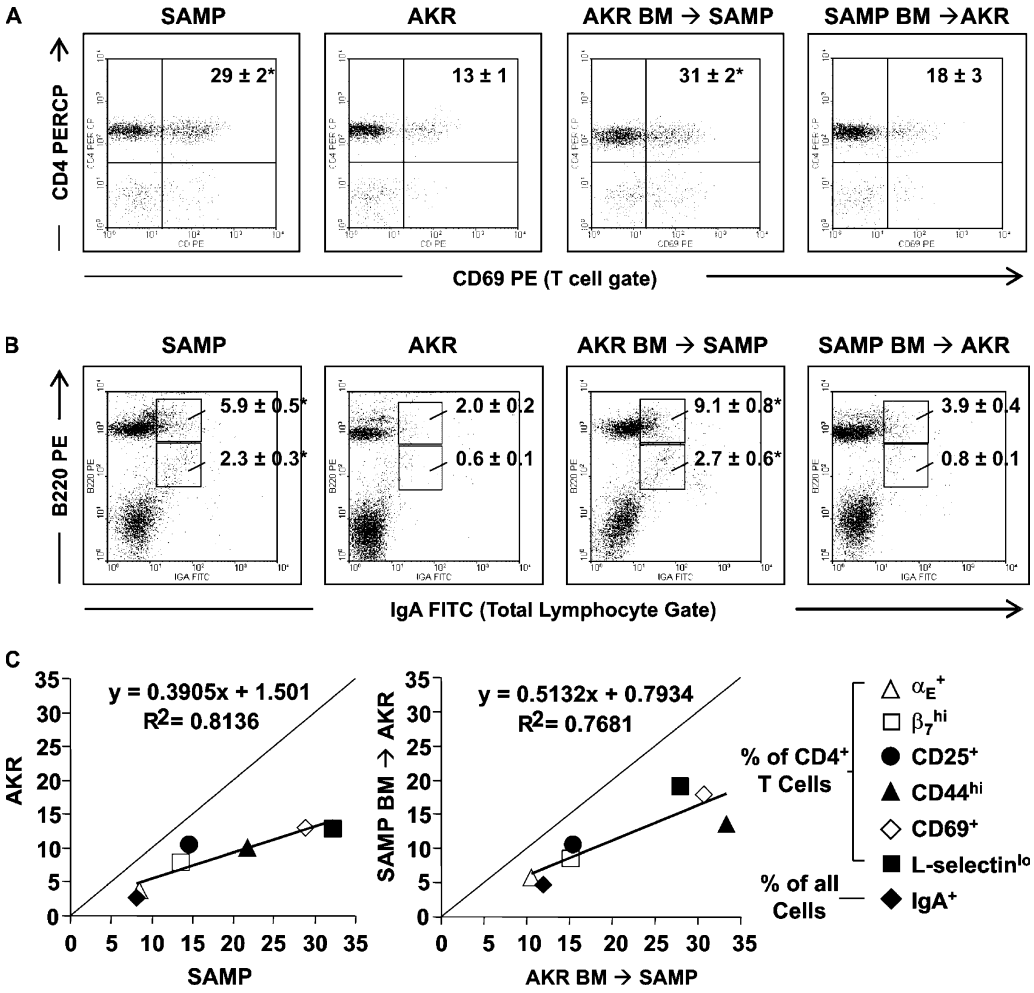

Figure 2. Inflammatory status of host determines pathogenicity and phenotype of MLN lymphocytes. Flow cytometry was performed on MLN lymphocyte populations in SAMP ($n = 3$), AKR ($n = 3$), AKR BM → SAMP ($n = 7$), and SAMP BM → AKR ($n = 6$) mice. (A) Representative T cell–gated ($CD4^+CD8^+$) dotplots of CD4 (y) versus CD69 (x) expression, with percentages of $CD4^+$ T cells that are $CD69^+$. (B) Representative dotplots of B220 (x) versus IgA (y) expression, with averages of IgA^+B220^{hi} mature B cells and IgA^+B220^{int} plasmablasts as a percentage of all lymphocytes. Results are expressed as mean ± SEM. *Indicates significantly increased ($P < 0.05$) compared with AKR or SAMP BM → AKR mice. Lymphocyte subsets that were significantly increased in SAMP (x) versus AKR (y) mice included the percentage of IgA^+ cells (◆) and the percentage of $CD4^+$ T cells that were α_E^+ (△), β_7^{hi} (□), $CD25^+$ (●), $CD44^{hi}$ (▲), $CD69^+$ (◇), and L-$selectin^{lo}$ (■) (C, left). Similar trends were seen in a plot of SAMP BM → AKR (y) versus AKR BM → SAMP (x) subsets (C, right). The slopes of the best-fit lines through the points in the two plots were not significantly different.

Size and pathogenicity of MLN lymphocyte subsets determined by inflammatory status of host

Given the extensive characterization of surface marker and cytokine expression differences between SAMP and AKR MLN populations in previous studies (36, 38) and the ability of SAMP MLN lymphocytes to transfer ileitis to SCID mice, we next examined lymphocyte populations in AKR BM → SAMP and SAMP BM → AKR MLN. In 6–12-wk-old mice used as BM donors, SAMP MLN had increased percentages of IgA^+ B cells (8.2 ± 0.8% versus 2.6 ± 0.3%, mean ± SEM) and $CD4^+$ T cells expressing the activation marker CD69 (29 ± 2% versus 13 ± 1%) relative to AKR MLN (Fig. 2, A and B). Interestingly, MLN from AKR BM → SAMP mice contained elevated percentages of $CD4^+$ T cells expressing CD69 (31 ± 2%) and IgA^+ B cells (12 ± 1%) similar to that seen in native SAMP MLN, even though the vast majority of MLN lymphocytes in AKR BM → SAMP mice are derived from AKR BM. Likewise, MLN from SAMP BM → AKR contained low percentages of $CD4^+$ T cells expressing CD69 and IgA^+ B cells, similar to the size of these populations in native AKR mice, even though MLN lymphocytes in SAMP BM → AKR mice are derived from SAMP BM. Furthermore, most of the other lymphocyte populations that were increased in SAMP relative to AKR MLN were also increased in AKR BM → SAMP MLN relative to SAMP BM → AKR MLN, including the percentage of $CD4^+$ T cells that are β_7 $integrin^{hi}$ (15 ± 1% versus 8 ± 2%), α_E $integrin^+$ (11 ± 1% versus 5.8 ± 0.7%), $CD25^+$ (15 ± 1% versus 11 ± 2%), L-$selectin^{lo}$

(33 ± 6% versus 14 ± 2%), and CD44^{hi} (28 ± 2 versus 19 ± 3%) (Fig. 2 C). Plotting the size of each of these lymphocyte populations in SAMP on the x axis relative to the size in AKR mice on the y axis, the best-fit linear regression through these points has a slope that is not significantly different from the linear regression of sizes of the same populations in a plot of AKR BM → SAMP on the x axis versus SAMP BM → AKR on the y axis (Fig. 2 C). In contrast, the slope of the regression line through these points when SAMP BM → AKR is plotted on the x axis and AKR BM → SAMP size is plotted on the y axis is significantly different ($P < 0.05$) compared with the slope of the regression line on the SAMP (x) versus AKR (y) plot. These data strongly suggest that the overall MLN composition of AKR BM → SAMP mice closely resembles that seen in SAMP mice, though most MLN cells in AKR BM → SAMP are derived from AKR mice. Likewise, the MLN composition of SAMP BM → AKR mice resembles that seen in AKR mice.

The aforementioned findings show that SAMP MLN lymphocyte population size is determined by the inflammatory status of the host and not by an intrinsic property of the lymphocytes themselves. Previous studies have shown that SAMP MLN CD4$^+$ T cells express more IFNγ and TNF than do AKR MLN CD4$^+$ T cells (36). To test whether the above redistribution of MLN lymphocyte subset size according to recipient inflammatory status is accompanied by a change in the inflammatory potential of SAMP- and AKR-derived CD4$^+$ T cells, we measured cytokine expression in MLN CD4$^+$ T cells cultured for 48 h in the presence of anti-CD3 stimulation (Fig. 3). Consistent with previous findings, SAMP MLN CD4$^+$ T cells exhibit an overall pattern of higher levels of cytokine production when compared with the cytokine profile of AKR cells. Compared with SAMP BM → AKR cells, AKR BM → SAMP CD4$^+$ T cells produced significantly more TNF and IFNγ, with the average expression being greater than 18- and 130-fold higher, respectively, in AKR BM → SAMP mice. AKR BM → SAMP cells also produce 15-fold higher levels of IL-2 than that produced by SAMP BM → AKR cells, suggesting that AKR BM → SAMP CD4$^+$ T cells may proliferate at a higher rate than SAMP BM → AKR cells. Furthermore, whereas SAMP BM → AKR produce little or no IL-4 and IL-5, AKR BM → SAMP T cells produce significantly greater amounts of both of these cytokines ($P < 0.05$), suggesting that T cells derived from AKR BM are capable of orchestrating both the Th1 and Th2 inflammatory responses that have been observed in native SAMP ileitis (37, 40). Interestingly, AKR BM → SAMP CD4$^+$ T cells produce even higher levels of cytokines than native SAMP T cells, which may account for the increased inflammatory scores in AKR BM → SAMP versus native SAMP mice. Although SAMP BM → AKR cells produce significantly higher IFNγ compared with levels produced by native AKR cells, overall differences in cytokine expression pattern between these two groups, measured by two-way ANOVA, were not significantly different. Increased cytokine expression by native SAMP and AKR BM → SAMP MLN CD4$^+$ T cells is not simply caused by global increases in bacterial translocation to the MLN in these mice, as there are no differences in bacterial load within the MLN of native SAMP versus AKR MLN or among the MLN from each of the transplant recipient groups (unpublished data).

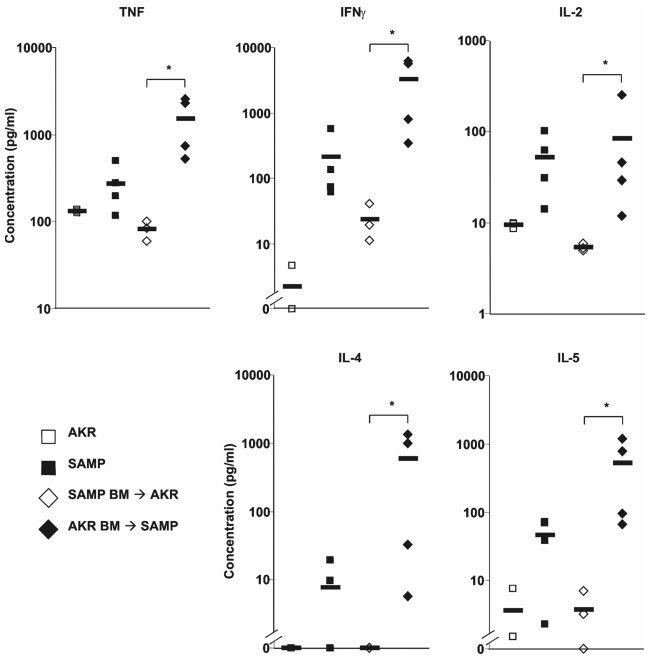

Figure 3. Increased cytokine expression in MLN CD4$^+$ T cells from AKR BM → SAMP mice. Levels of secreted TNF, IFNγ, IL-2, IL-4, and IL-5 were measured in triplicate by cytometric bead array, from 48-h cultures of AKR (□, $n = 3$), SAMP (■, $n = 4$), SAMP BM → AKR (△, $n = 3$), and AKR BM → SAMP (▲, $n = 4$) MLN CD4$^+$ T cells (10^5/well), stimulated with immobilized anti-CD3 antibody. Points represent individual mice with the mean value (_) in each group also shown. *Significantly increased compared with SAMP BM → AKR cells ($P < 0.05$).

SAMP and AKR BM → SAMP mice exhibit epithelial barrier dysfunction

To investigate whether epithelial dysfunction may be responsible for the nonhematopoietic ileitis susceptibility trait in SAMP mice, we measured ileal epithelial permeability to charged ions in ilea of experimental mice using a previously described transepithelial electrical resistance (TEER) assay (44). Although ilea from AKR mice maintained their baseline TEER after 1 h of culture (ΔTEER at 1 h, 2 ± 3 Ω.cm^2, mean ± SEM), SAMP ilea exhibited a substantial drop in TEER during the same time period (−8 ± 1 Ω.cm^2), suggesting that SAMP epithelium may not be able to maintain an effective permeability barrier (Fig. 4 A, left). Ilea from AKR BM → SAMP mice also exhibited a decrease in TEER at 1h (−5 ± 1 Ω.cm^2), whereas SAMP BM → AKR ilea maintained their baseline TEER levels (0 ± 1 Ω.cm^2), suggesting that the epithelial permeability defect in SAMP mice is not dependent on the specific attributes or factors produced preferentially by SAMP hematopoietic cells.

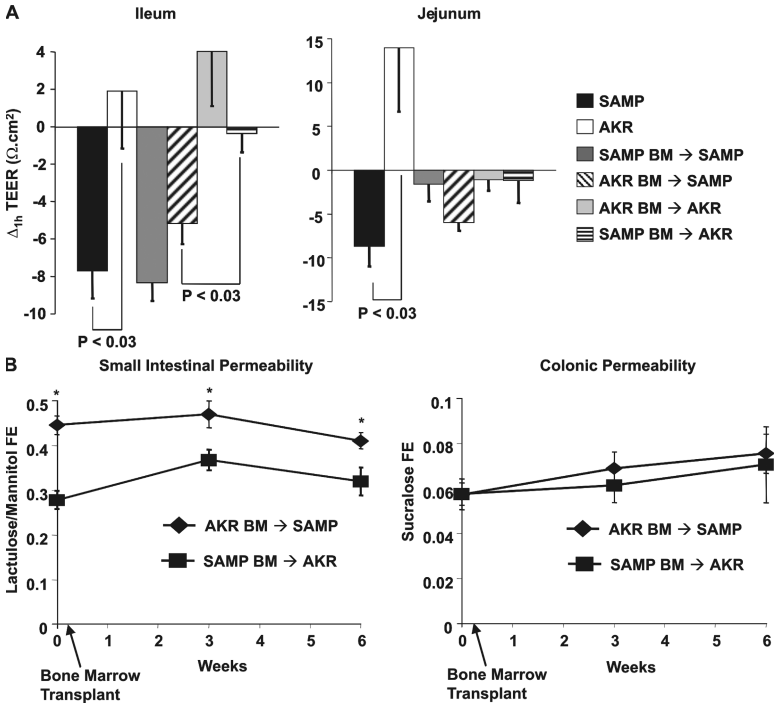

Figure 4. Epithelial barrier dysfunction in SAMP and AKR BM → SAMP mice. (A) TEER assays on ileum and jejunum from SAMP ($n = 8$), AKR ($n = 8$), SAMP BM → SAMP ($n = 5$), AKR BM → SAMP ($n = 4$), AKR BM → AKR ($n = 3$), and SAMP BM → AKR ($n = 4$) mice. Ilea from SAMP, SAMP BM → SAMP, and AKR BM → SAMP mice exhibited decreases in ΔTEER indicative of increased epithelial permeability, whereas ilea from AKR, AKR BM → AKR, and SAMP BM → AKR mice maintained an effective epithelial resistance barrier. Significant differences ($P < 0.03$) are indicated between experimental groups (A, left). No differences were observed in jejunal TEER among BMT recipient groups. A significant in crease in TEER was seen in native SAMP compared with AKR jejunum; $P < 0.03$ (A, right). (B) In vivo assays measuring epithelial permeability to solutes in the small intestine and colon using urinary FE ratio of lactulose to mannitol (B, left) and of sucralose (B, right), respectively, in AKR BM → SAMP (◆) ($n = 6$) and SAMP BM → AKR (■) ($n = 6$) mice. The time 0 point was collected immediately before irradiation and transplantation and thus represent the permeability of native SAMP (◆) and AKR (■) tissues. *Indicates significantly increased ($P < 0.05$) compared with SAMP BM → AKR mice.

Increased epithelial permeability was also seen in the jejunum of native SAMP (-9 ± 2) versus native AKR (14 ± 7), though no differences in ΔTEER were seen among the four transplant recipient groups (Fig. 4 A, right). No jejunal inflammation was detectable in native SAMP mice or in any of the transplant recipient groups. The discrepancy between the presence of the epithelial permeability defect in both jejunum and ileum and the restriction of inflammation to the ileum in native SAMP mice may be explained by differential bacterial load, as SAMP ileal bacterial load was increased >10-fold compared with jejunum (unpublished data). Given that inflammation in native SAMP mice is decreased by antibiotic treatment (40) and that inflammation in transplant recipients can be reduced > 70% by continuous posttransplant antibiotic therapy (unpublished data), the high bacterial load present in the ileum is likely required, along with epithelial barrier dysfunction, to initiate inflammation.

To examine epithelial permeability in vivo and to determine the specific sites along the gastrointestinal tract that may display an epithelial permeability defect in SAMP and AKR BM → SAMP mice, we gave AKR BM → SAMP and SAMP BM → AKR mice an orogastric gavage of a disaccharide probe containing sucrose, lactulose, mannitol, and sucralose before and for several weeks after BMT. We then analyzed the fractional excretion (FE) of these sugars in the 24-h period after probe administration to determine epithelial permeability in specific regions in the gastrointestinal tract as previously described (45). Before receiving irradiation and BM transplant, SAMP mice (AKR BM → SAMP, time 0) had elevated lactulose to mannitol FE ratios relative to AKR mice (SAMP BM → AKR, time 0) (lactulose FE/mannitol FE, 0.44 ± 0.02 versus 0.28 ± 0.02, mean ± SEM), indicative of increased small intestinal epithelial permeability in SAMP mice (Fig. 4 B, left). AKR BM → SAMP mice also displayed increased epithelial permeability in the small intestine relative to SAMP BM → AKR mice both 3 wk (0.47 ± 0.03 versus 0.37 ± 0.02, mean ± SEM) and 6 wk (0.41 ± 0.02 versus 0.32 ± 0.03) after transplant. In contrast, no differences were measured in the FE of sucralose, an indicator of colonic permeability, among SAMP, AKR, AKR BM → SAMP, and SAMP → AKR mice (Fig. 4 B, right).

Increased epithelial permeability precedes the onset of inflammation and is present in the absence of bacterial

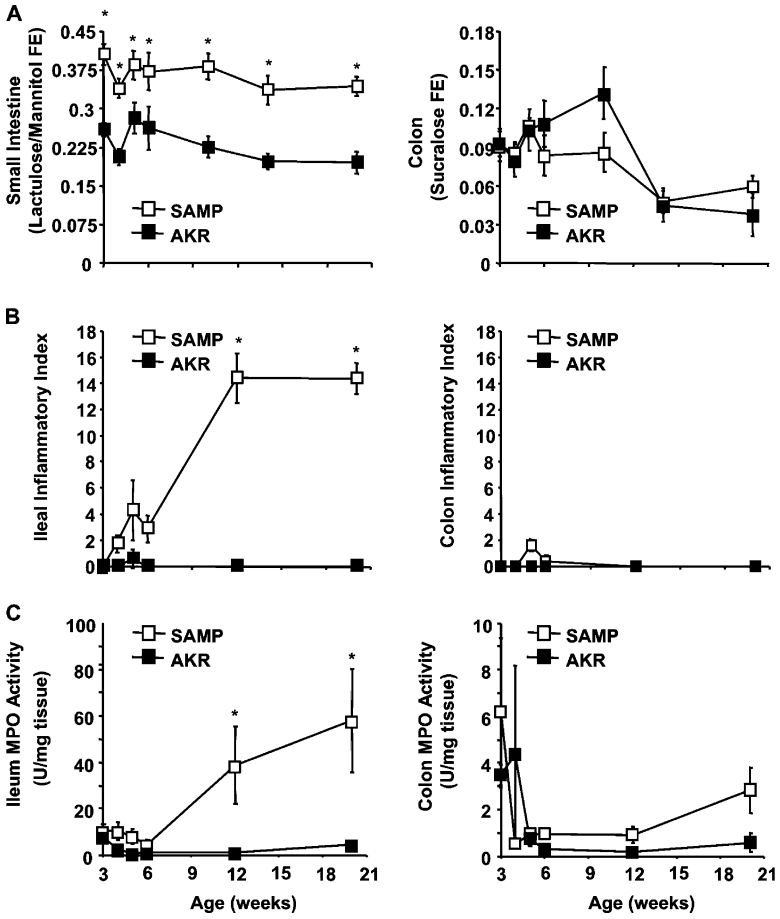

Figure 5. Increased small intestinal permeability occurs before the onset of inflammation in SAMP mice. (A) Paracellular permeability, measured in the small intestine and colon using the in vivo probe assay, was increased as early as 3 wk of age in SAMP (□) compared with age-matched AKR (■) mice, and remained elevated through 20 wk. (B) Total inflammatory scores for the ileum and colon show that inflammation was not significantly increased in SAMP versus AKR ileum until 12 wk of age. (C) Ileal MPO activity, providing a quantitative marker of active inflammation, showed a strong correlation with histologic ileal inflammatory score ($r = 0.77$) and was also not increased in SAMP versus AKR mice until 12 wk. $n \geq 4$ per group; *$P < 0.05$ versus age-matched AKR.

colonization in SAMP mice. The epithelial barrier defect was further characterized by measuring intestinal epithelial permeability using the aforementioned in vivo disaccharide probe method in native SAMP and AKR mice beginning at 3 wk of age, immediately after weaning, and continuing at specified intervals through 20 wk of age. SAMP mice exhibited a 1.6-fold higher small intestinal permeability than age-matched AKRs throughout the time course studied (Fig. 5 A, left), with the increased permeability relative to AKR present even at the earliest time point assayed. In a parallel time course study measuring total ileal inflammation by histologic score (Fig. 5 B, left) and acute inflammation/neutrophil infiltration by myeloperoxidase (MPO) assay (Fig. 5 C, left), 3-wk-old SAMP ilea displayed no histologic evidence of inflammation and only low levels of MPO activity that were not greater than levels measured in 3-wk-old AKR ilea. Furthermore, inflammatory scores and MPO activity were not considerably greater in SAMP compared with AKR mice until after 6 wk of age. Thus, increased epithelial permeability precedes the development of inflammation in SAMP mice by at least 3 wk. In contrast to the small intestine, no differences in AKR versus SAMP colonic permeability were seen at any age studied, and neither SAMP nor AKR mice displayed histologically detectable colitis or high levels of MPO activity throughout this time course (Fig. 5, A–C, right).

Small intestinal permeability in 3-wk-old SAMP mice raised under GF conditions was nearly identical to that in age-matched SAMPs raised under specific pathogen-free (SPF) conditions (0.40 ± 0.06 vs. 0.41 ± 0.02, NS), but significantly greater than (1.55-fold) small intestinal permeability in age-matched, SPF-raised AKR mice (0.26 ± 0.01, $P < 0.05$) (Fig. 6 A). Mice from all of these groups displayed normal bowel wall architecture with histologic inflammatory scores close to zero (Fig. 6). Thus, increased epithelial permeability in SAMP mice occurs independently from colonization with commensal bacteria.

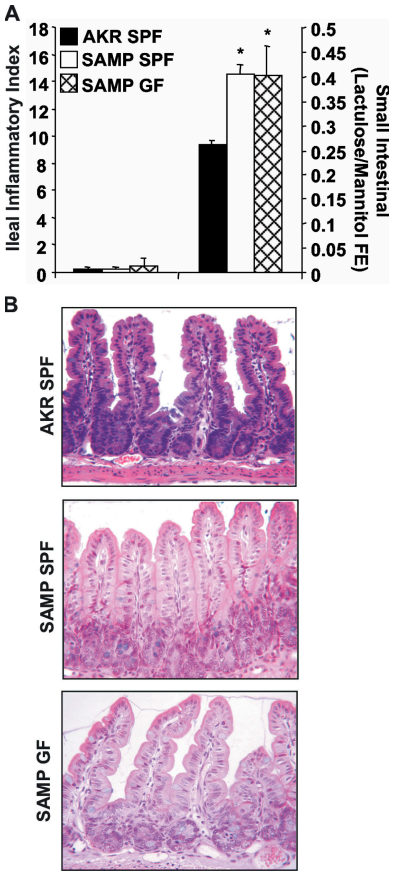

Figure 6. Early, preinflammatory alterations in small intestinal barrier function persist in the absence of the enteric flora. (A) Small intestinal paracellular permeability in GF SAMP mice was similar to permeability in SAMP mice raised under SPF conditions, and significantly increased compared with SPF-AKR permeability $n \geq 4$ per group; *$P < 0.05$ versus age-matched AKR. (B) 3-wk-old GF SAMP mice displayed no histological signs of ileal inflammation and possessed normal intestinal architecture.

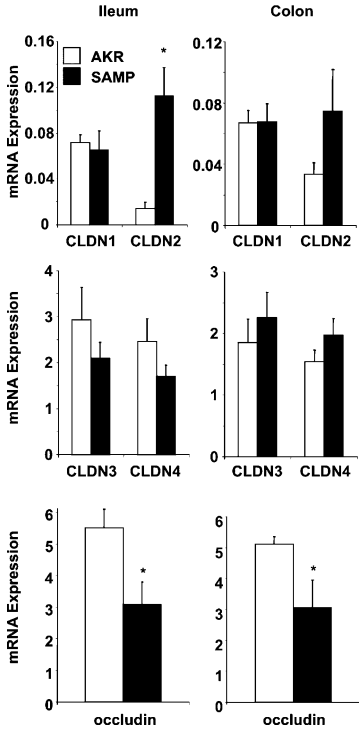

Figure 7. Altered epithelial TJ protein expression in young, uninflamed SAMP compared with AKR mice. mRNA transcript levels of TJ proteins (claudin [CLDN] 1–4 and occludin) were measured by RT-PCR and expressed relative to HGPRT in isolated intestinal epithelial cell preparations from the ileum (left) or colon (right) of SAMP and AKR mice (3 wk of age; $n \geq 4$ animals per group). The greatest differences in expression in SAMP ileum compared with age-matched AKR controls were seen in CLDN2 (eightfold increase; top left) and occludin (1.8-fold decrease; bottom left). Similar trends were seen in the colon, though increases in CLDN2 (top right) expression in SAMP versus AKR colon were not statistical significant. No differences in expression were noted for CLDN1, 3, and 4 in either the ileum or colon of SAMP relative to controls. $n \geq 4$ per group; *$P < 0.05$ versus control AKR.

Altered TJ protein expression in SAMP ileum accompanies epithelial permeability defect

To begin to elucidate potential mechanism(s) underlying the epithelial permeability defect in SAMP ileum, expression of TJ-associated ZO-1, claudin-1, -2, -3, and -4, and occludin was characterized in 3-wk-old SAMP and AKR mice. Immunohistochemical examination of ZO-1 in SAMP ileum and colon demonstrated perijunctional staining with no notable differences in ZO-1 staining compared with AKR controls (unpublished data). Claudin-1, -3 and -4 mRNA levels were expressed at comparable levels in isolated epithelial cells from 3-wk-old SAMP versus AKR ileum as well as colon (Fig. 7). Claudin-2 mRNA expression, however, was found to be more than eightfold greater in SAMP versus AKR ileum. Although an increased trend in claudin-2 mRNA expression was observed in SAMP versus AKR colon, this increase was not statistically different. Conversely, an ~1.8-fold decrease in occludin expression was found in SAMP versus AKR ileum as well as colon (Fig. 7). These data suggest that although decreased expression of occludin is present in both the ileum and colon of SAMP compared with AKR, the epithelial permeability defect may be heightened in combination with the high levels of claudin-2 expression in the ileum, but not the colon, of SAMP mice.

DISCUSSION

The presence of severe ileitis in SAMP mice reconstituted with AKR BM, but not in AKR mice reconstituted with SAMP BM, demonstrates that the primary factor responsible for the induction of ileitis in SAMP mice originates within a nonhematopoietic tissue. As a corollary, this finding also establishes that AKR hematopoietic cells transplanted into SAMP do not prevent ileitis, but rather orchestrate an ileal inflammatory response with similar severity to that produced by SAMP hematopoietic cells, confirming previous results suggesting that SAMP ileitis is not caused by defects in SAMP

regulatory T cell function (38). Further, we have demonstrated that when transplanted into SAMP mice, certain subpopulations of AKR MLN lymphocytes expand to approximate the sizes of these populations in SAMP mice. Many of these subsets, including α_E^+ $CD4^+$ T cells and $CD25^+$ $CD4^+$ T cells may represent activated and/or regulatory T cell populations (38). Therefore as demonstrated in our previous studies, it is possible that, like SAMP regulatory cells, AKR regulatory cells may expand as part of a futile compensatory effort to curb ileal inflammation characteristic of SAMP mice.

In addition to regulatory cell expansion, some AKR $CD4^+$ T cells in AKR BM → SAMP mice also acquire increased pathogenicity, because they not only participate in the severe inflammation seen in AKR BM → SAMP mice, but they also transfer significantly more severe ileitis to SCID mice than do $CD4^+$ T cells from native AKR mice (unpublished data). This pathogenicity is likely linked to the elevated cytokine production exhibited by AKR-derived $CD4^+$ T cells in AKR BM → SAMP mice. Interestingly, SAMP $CD4^+$ T cells from SAMP BM → AKR mice still transfer ileitis to SCID mice, despite the fact that these cells don't produce ileitis in SAMP BM → AKR mice themselves (unpublished data). One possible explanation for this discrepancy is that the small population of mature $CD4^+$ T cells present in BM (46) may have been transplanted into AKR mice along with SAMP hematopoietic stem cells, and that the progeny of this preprogrammed inflammatory population may be present in the MLN $CD4^+$ T cell population transferred to SCID mice. Alternatively, SAMP T cells may possess intrinsically more potent ileitis-producing capacity than AKR T cells and are thus still able to induce ileitis in SCID mice even after undergoing reeducation in AKR mice. Regardless, $CD4^+$ T cells from SAMP BM → AKR mice produce low overall levels of cytokines similar to that produced by native AKR $CD4^+$ T cells. Thus, if SAMP-derived $CD4^+$ T cells do possess increased ileitis-promoting capacity, this capacity appears to be suppressed in the AKR host and must be reacquired upon transfer of these SAMP-derived cells from AKR to SCID mice. Thus, the nonhematopoietic-derived resistance to ileitis in AKR mice is dominant over any leukocyte-derived susceptibility. Given previous reports of epithelial dysfunction caused by the deficient immune system in SCID mice (47), we speculate that SCID mice may also possess a nonhematopoietic ileitis susceptibility factor, enabling transferred AKR BM → SAMP, SAMP BM → AKR, or native SAMP $CD4^+$ T cells to induce severe inflammation.

The epithelial barrier defect seen in SAMP and AKR BM → SAMP mice suggests that epithelial cell dysfunction may be primarily responsible for the development of ileitis in this model. Because epithelial barrier dysfunction can be induced by proinflammatory cytokines (48), it remains to be definitively proven whether the epithelial permeability defect observed in SAMP mice is a cause or a consequence of ileitis in this model. For instance, TNF and IFNγ induce large increases in intestinal permeability of intestinal epithelial cell lines through NF-κB transcriptional activation resulting in redistribution of ZO-1, claudins, and occludin from the junctional interface to the cytoplasm (31, 48). However, we have shown that this permeability defect is not dependent on strain-specific proinflammatory properties of SAMP leukocytes, as AKR BM → SAMP mice also exhibit this epithelial permeability defect. Furthermore, considerable epithelial barrier dysfunction was found even in 3-wk-old SAMP mice, an age by which ileal inflammation has not yet developed, providing convincing evidence in favor of the primacy of barrier dysfunction as an etiologic factor in SAMP ileitis. Interestingly, colonic epithelium exhibited normal barrier function compared with WT mice, a finding that may explain the lack of colonic inflammation in this model. Native SAMP jejunal epithelium does appear to possess the permeability defect, though the lower bacterial load in the jejunum versus the ileum may explain why inflammation is primarily limited to the ileum.

Barrier dysfunction can also be produced directly by both pathogenic and commensal bacterial through a variety of mechanisms. For example, enteropathogenic *E. coli* induces dephosphorylation and tight junctional dissociation of occludin thereby increasing permeability (30). However, unlike other models of inflammatory bowel disease such as the $IL\text{-}10^{-/-}$ model, in which commensal flora interactions are required for increases in colonic permeability that precede inflammatory changes (49), our study shows that increased ileal epithelial permeability in SAMP mice occurs to the same extent in GF animals without evidence of colonization. Importantly, defects intrinsic to other cell types, such as stromal cells, that also play roles in modulating epithelial permeability (27) could also cause this barrier defect and through cell–cell interactions may cause the altered TJ membrane protein expression observed in SAMP mice. Additionally, we cannot exclude involvement of residual recipient macrophages and dendritic cells in the ileitis seen in AKR → SAMP mice. However, the ileitis in SAMP mice is unlikely to result from intrinsic properties of these antigen-presenting cells, because these cells are incapable of producing inflammation in SAMP BM → AKR mice.

SAMP ilea possess many abnormalities in epithelial appearance and composition that have been previously reported (34). Further studies demonstrated markedly expanded and aberrant rearrangement of secretory lineage Paneth and goblet cell populations in SAMP ileum (36), similar to epithelial phenotype changes observed in human CD (50), which may contribute to increased epithelial permeability. Data in the present study demonstrate that TJ protein expression is also altered in SAMP versus AKR ileum. Although barrier dysfunction produced by infection in vivo (51) or inflammatory mediators in vitro (31) involves relocalization of ZO-1, no abnormal localization of ZO-1 was noted in SAMP ileum, suggesting that the high epithelial permeability in SAMP mice may not be caused by reorganization of cytoskeletal connections with TJs. Global decreases in intestinal occludin mRNA and protein expression have been observed in CD patients (52). Given the fact that down-regulation of occludin has been shown to increase epithelial permeability (30), it is likely that the decreased

occludin expression we have observed in SAMP versus AKR ileum may contribute to barrier dysfunction in SAMP mice. Although high levels of occludin and some claudin isoforms enhance epithelial barrier function through stabilization of TJs, increased claudin-2 expression has been shown in an in vitro transfection system to increase epithelial permeability, possibly by forming lower affinity interactions with other claudin isoforms on neighboring cells (28). Thus, the increased claudin-2 expression by SAMP versus AKR epithelial cells may also contribute to the defective barrier phenotype.

In conclusion, we have demonstrated that the primary susceptibility leading to the development of ileitis in SAMP mice is derived from a nonhematopoietic source, as SAMP BM progenitor cells do not transmit this ileitis phenotype when transplanted into AKR mice. Further, we have shown that hematopoietic cells from normal mice transplanted into SAMP mice can fully orchestrate this ileal inflammatory response in the presence of this nonhematopoietic susceptibility, acquire surface phenotypes similar to cells seen in native SAMP, and undergo maturation and reeducation such that T cells derived from these AKR cells express high levels of inflammatory cytokines. Epithelial barrier dysfunction in native SAMP mice and SAMP mice reconstituted with AKR BM suggests that the epithelium may be responsible for this nonhematopoietic ileitis susceptibility, as barrier dysfunction precedes inflammation development by $>$ 3 wk and occurs in the absence of bacterial colonization. This barrier dysfunction may result from dysregulation of TJ proteins caused by aberrant intracellular signaling pathways possibly involving transcription factors such as Pparγ. Further studies that definitively prove that epithelial-specific dysfunction is the primary defect causing ileitis and uncover the specific molecular mechanisms leading to loss of barrier integrity are warranted and may provide critical insights into the etiology of CD.

MATERIALS AND METHODS

Animal model. SAMP mice were propagated at the University of Virginia, with founders provided by S. Matsumoto (Yakult Central Institute for Microbiological Research, Tokyo, Japan), and originally derived from the AKR/J strain (Jackson Laboratories). SAMP and WT AKR mice were housed under SPF at the UVA. GF SAMP were derived and maintained at Taconic Farms (Rockville, MD), and shipped in sterile isolators and used in experiments upon arrival. All mice were maintained in accordance to approved protocols by the Institutional Animal Care and Use Committee and Association for Assessment of Laboratory Animal Care.

BM transplantation. Mice receiving BMT were irradiated (600 RAD) on the morning of transplantation and 4–6 h later, immediately before transplantation. BM was harvested from femurs and tibias of 6-wk-old SAMP or AKR mice with RPMI (10% FCS), and cell suspensions washed and diluted to a concentration of 30×10^6 cells/ml in HBSS. 7.5×10^6 cells/250 μl were injected i.v. into the lateral tail veins of recipient mice. BMT mice were placed on antibiotic water (0.7 mM neomycin sulfate, 80 mM sulfamethoxazole, and 0.37 mM trimethoprim) for 2 wk after irradiation, and then given autoclaved water to reconstitute normal gut flora.

Histology. The distal 10 cm of ileum from experimental mice was removed, flushed of fecal contents, opened longitudinally, and placed in Bouin's fixative. Tissues were embedded in paraffin, cut to 3 μm, and stained with hematoxylin and eosin. Ileitis severity was assessed by a trained pathologist in a blinded fashion using an established histologic scoring system (43), wherein total inflammatory index represents the sum of three individual indices: active inflammation, chronic inflammation, and villous distortion as described in detail elsewhere (43).

Flow cytometry. MLN from experimental mice were homogenized through 70-μm strainers into PBS containing 2% FBS. 10^6 cells/sample were stained with combinations of FITC-, PE-, PERCP-, and APC-labeled hamster anti–mouse CD69 (H1.2F3) and rat anti–mouse CD4 (RM4-5), CD19 (1D3), B220 (RA3-6B2), IgA (C10-3), α_E integrin (M290), β_7 integrin (M293), CD25 (PC61), CD44 (IM7), and L-selectin (MEL-14) (BD PharMingen). Excess antibody was removed and cells fixed in 2% paraformaldehyde before analysis by FACS, with postrun data analyzed using WinMidi 2.8 (Trotter).

Cell culture. $CD4^+$ T cells from experimental mice were cultured in 96-well plates coated with anti–mouse CD3 (1 μg/ml, clone 145-2C11; BD PharMingen) at 37°C with 5% CO_2 in RPMI (10% FCS, 100 U/ml penicillin, 100 μg/ml streptomycin, 1 mM sodium pyruvate, 1 mM nonessential amino acids, 50 μM 2β-mercaptoethanol) for 48 h at 10^5 cells/well in 100 μl. Undiluted supernatants were assayed for TNF, IFNγ, IL-2, IL-4, and IL-5 using the mouse Th1/Th2 cytokine kit (BD PharMingen) according to manufacturer's instructions.

Ex vivo permeability. TEER assays were performed after a previously published method (44). In brief, distal ilea from experimental mice were removed, flushed with 0.9% NaCl, and opened longitudinally to expose mucosal surfaces. Two 3-mm squares of tissue were excised and placed apical side up on separate precut and wetted 0.4-μm pore size membranes (Costar Corning Inc.). Specimens were mounted between two custom made Plexiglass discs with laser cut holes (2-mm diameter) to expose apical and basolateral tissue surfaces, inserted into a Snapwell (Costar) apical side up, and fitted into a 6-well plate with 3 ml DMEM (glutamine, nonessential amino acids, 100 U/ml penicillin, and 100 μg/ml streptomycin) added basally and 300 μl apically. TEER readings were taken using an EVOM voltmeter with an EndOhm chamber attachment (World Precision Instruments) immediately after assembling transwell apparati and after 1 h incubation at 37°C. Baseline resistance readings were determined in transwells containing membrane inserts only and subtracted from sample values.

In vivo permeability. Experimental mice were assayed in vivo for intestinal permeability using a previously established method (45, 51). In brief, mice were fasted for 2 h before oral gavage of disaccharide permeability probes (500 mg/ml sucrose, 60 mg/ml lactulose, 40 mg/ml mannitol, 30 mg/ml sucralose in 0.2 ml water), and placed into individual metabolic cages (Nalge Nunc Int.) for 22 h to allow for urine collection, which was gravimetrically determined and recorded. Concentration of sucrose, lactulose, and mannitol in specimens was determined by pulsed amperometric detection using a Dionex HPLC with MA-1 columns (Dionex) and NaOH-based elution (45). Similarly, sucralose concentrations were determined using Dionex Ionpac NS1 columns (Dionex) and a gradient of acetonitrile in water as the eluent for HPLC analysis (45). Data were expressed as urinary FE.

MPO assay. Ileum and colon samples were assayed for MPO activity as previously described (53, 54). Specimens were collected, weighed, diluted 20-fold in 0.5% HTAB buffer, homogenized with a Polytron PT 10–35 tissue homogenizer (Kinematica), and centrifuged to pellet debris. Samples (7 μL) were loaded in triplicate into a 96-well plate and exposed to substrate solution (200 μL; 5 mM potassium phosphate buffer containing 0.0005% H_2O_2 and 0.167 mg/ml O-dianisidine). The average rate of absorbance change at 450 nm over 2 sequential 30-s intervals was used to calculate MPO activity.

mRNA expression of TJ proteins. Expression of occludin and claudins-1 to -4 mRNA transcripts in primary epithelial cell isolations relative to

hypoxanthine-guanine phosphoribosyl transferase (HGPRT; housekeeper) was performed using the following primers: occludin sense (5′-CCCTG-ACCACTATGAAACAG-3′) and antisense (5′-TTGATCTGAAGTGA-TAGGTG-3′); claudin-1 sense (5′-ACGGTCTTTGCACTTTGGT-3′) and antisense (5′-AGTTTGCAGGATCTGGGAT-3′); claudin-2 sense (5′-TATCTGTGTGGTGGGCATGA-3′) and antisense (5′-CGAAGGA-TGCCATGAAGATT-3′); claudin-3 sense (5′-CCACTACCAGCAGT-CGATGA-3′) and antisense (5′-CAGCCTGTCTGTCCTCTTCC-3′); claudin-4 sense (5′-AGCAAACGTCCACTGTCCTT-3′) and antisense (5′-CCCTCATCAGTCACTCAGCA-3′); and HGPRT sense (5′-TGC-CGAGGATTTGGAAAAAGTG-3′) and antisense (5′-CACAGAGGGCC-ACAATGTGATG-3′). Real-time PCR was performed using a Bio-Rad iCycler iQ Real Time Detection system and software (Bio-Rad Laboratories). Reaction mixture consisted of final concentrations of 1× PCR buffer, 200 μM dATP, dCTP, dGTP, and dTTP, 3 mM $MgCl_2$, 0.5 U Platinum Taq polymerase, and 400 nM of each primer in a 25 μl volume. Thermal cycling conditions were 95°C/2 min followed by 40 cycles of 95°C/15 s, 60°C/15 s, and 72°C/15 s. Expression of occludin and claudins-1 through −4 were normalized to HGPRT mRNA.

Statistics. Statistical analysis was performed using the two-tailed Student's *t* test, with statistical significance set at $P < 0.05$. Coefficients of determination, R^2, were determined by linear regression. Statistical comparison of the slopes of linear regression correlations was performed using the formula: t statistic = (b1−b2)/S(b1−b2), where b1 and b2 are the slopes of the lines and S(b1−b2) is the standard error of the difference of the regression slopes. This t statistic was compared with the critical t stat for the relevant degrees of freedom using $P < 0.05$ to determine significance. Statistical comparisons of cytokine expression were performed using two-way analysis of variance on ranks (Friedman's Test), using mouse strain as one factor and cytokine expression as the other factor. The Holm-Sidak adjustment for multiple comparisons was then used to make pairwise comparisons between mouse strains in terms of individual cytokine production.

The authors would like to acknowledge Drs. Christopher Moskaluk and James Mize for histopathologic evaluation, Kim Tran for HPLC analysis, William Ross for flow cytometry expertise, Matt Staples, Angela Best, Anthony Bruce, and Robert Knight for technical assistance, and Dr. Satoshi Matsumoto for providing original SAMP1/Yit breeding pairs.

This work was supported by National Institutes of Health P01DK57880 (to F. Cominelli, S.M. Cohn, K.F. Ley, and T.T. Pizarro), R01DK56762 (to T.T. Pizarro), K26RR00175 (to P.B. Ernst), GM07267-23 (University of Virginia to T.S. Olson), and the Morphology/Imaging (Sharon Hoang and Greg Harp) and Immunology Cores of the National Institutes of Health-funded Silvio O. Conte Digestive Diseases Research Center at University of Virginia, P30DK56703 (to F. Cominelli/T.T. Pizarro and F. Cominelli/P.B. Ernst). Additional support was provided by the Crohn's & Colitis Foundation of America (to B.K. Reuter), and a Fellowship from the Canadian Association of Gastroenterologists and Canadian Institute for Health Research (to K.G-E. Scott).

The authors have no conflicting financial interests.

Submitted: 22 February 2005
Accepted: 26 January 2006

REFERENCES

1. Bouma, G., and W. Strober. 2003. The immunological and genetic basis of inflammatory bowel disease. *Nat. Rev. Immunol.* 3:521–533.
2. Egan, L.J., and W.J. Sandborn. 2004. Advances in the treatment of Crohn's disease. *Gastroenterology*. 126:1574–1581.
3 Ma, T.Y. 1997. Intestinal epithelial barrier dysfunction in Crohn's disease. *Proc. Soc. Exp. Biol. Med.* 214:318–327.
4. Shanahan, F. 2002. Crohn's disease. *Lancet*. 359:62–69.
5. Ogura, Y., N. Inohara, A. Benito, F.F. Chen, S. Yamaoka, and G. Nunez. 2001. Nod2, a Nod1/Apaf-1 family member that is restricted to monocytes and activates NF-kappaB. *J. Biol. Chem.* 276:4812–4818.
6. Hisamatsu, T., M. Suzuki, H.C. Reinecker, W.J. Nadeau, B.A. McCormick, and D.K. Podolsky. 2003. CARD15/NOD2 functions as an antibacterial factor in human intestinal epithelial cells. *Gastroenterology*. 124:993–1000.
7. Monteleone, G., L. Biancone, R. Marasco, G. Morrone, O. Marasco, F. Luzza, and F. Pallone. 1997. Interleukin 12 is expressed and actively released by Crohn's disease intestinal lamina propria mononuclear cells. *Gastroenterology*. 112:1169–1178.
8. Fuss, I.J., M. Neurath, M. Boirivant, J.S. Klein, C. de la Mott, S.A. Strong, C. Fiocchi, and W. Strober. 1996. Disparate CD4+ lamina propria (LP) lymphokine secretion profiles in inflammatory bowel disease. Crohn's disease LP cells manifest increased secretion of IFN-gamma, whereas ulcerative colitis LP cells manifest increased secretion of IL-5. *J. Immunol.* 157:1261–1270.
9. Mottet, C., H.H. Uhlig, and F. Powrie. 2003. Cutting edge: cure of colitis by CD4(+)CD25(+) regulatory T cells. *J. Immunol.* 170: 3939–3943.
10. Powrie, F., M.W. Leach, S. Mauze, L.B. Caddle, and R.L. Coffman. 1993. Phenotypically distinct subsets of CD4+ T cells induce or protect from chronic intestinal inflammation in C. B-17 scid mice. *Int. Immunol.* 5:1461–1471.
11. Singh, B., S. Read, C. Asseman, V. Malmstrom, C. Mottet, L.A. Stephens, R. Stepankova, H. Tlaskalova, and F. Powrie. 2001. Control of intestinal inflammation by regulatory T cells. *Immunol. Rev.* 182: 190–200.
12. Kraus, T.A., L. Toy, L. Chan, J. Childs, and L. Mayer. 2004. Failure to induce oral tolerance to a soluble protein in patients with inflammatory bowel disease. *Gastroenterology*. 126:1771–1778.
13. Duchmann, R., I. Kaiser, E. Hermann, W. Mayet, K. Ewe, and K.H. Meyer zum Buschenfelde. 1995. Tolerance exists towards resident intestinal flora but is broken in active inflammatory bowel disease (IBD). *Clin. Exp. Immunol.* 102:448–455.
14. Kazemi-Shirazi, L., C.H. Gasche, S. Natter, A. Gangl, J. Smolen, S. Spitzauer, P. Valent, D. Kraft, and R. Valenta. 2002. IgA autoreactivity: a feature common to inflammatory bowel and connective tissue diseases. *Clin. Exp. Immunol.* 128:102–109.
15. Dohi, T., K. Fujihashi, T. Koga, Y. Shirai, Y.I. Kawamura, C. Ejima, R. Kato, K. Saitoh, and J.R. McGhee. 2003. T helper type-2 cells induce ileal villus atrophy, goblet cell metaplasia, and wasting disease in T cell-deficient mice. *Gastroenterology*. 124:672–682.
16. Dieckgraefe, B.K., and J.R. Korzenik. 2002. Treatment of active Crohn's disease with recombinant human granulocyte-macrophage colony-stimulating factor. *Lancet*. 360:1478–1480.
17. Lopez-Cubero, S.O., K.M. Sullivan, and G.B. McDonald. 1998. Course of Crohn's disease after allogeneic marrow transplantation. *Gastroenterology*. 114:433–440.
18. Cario, E., and D.K. Podolsky. 2000. Differential alteration in intestinal epithelial cell expression of toll-like receptor 3 (TLR3) and TLR4 in inflammatory bowel disease. *Infect. Immun.* 68:7010–7017.
19. Pizarro, T.T., M.H. Michie, M. Bentz, J. Woraratanadharm, M.F. Smith Jr., E. Foley, C.A. Moskaluk, S.J. Bickston, and F. Cominelli. 1999. IL-18, a novel immunoregulatory cytokine, is up-regulated in Crohn's disease: expression and localization in intestinal mucosal cells. *J. Immunol.* 162:6829–6835.
20. Dwinell, M.B., P.A. Johanesen, and J.M. Smith. 2003. Immunobiology of epithelial chemokines in the intestinal mucosa. *Surgery*. 133:601–607.
21. Meddings, J. 2000. Barrier dysfunction and Crohn's disease. *Ann. NY Acad. Sci.* 915:333–338.
22. Hollander, D., C.M. Vadheim, E. Brettholz, G.M. Petersen, T. Delahunty, and J.I. Rotter. 1986. Increased intestinal permeability in patients with Crohn's disease and their relatives. A possible etiologic factor. *Ann. Intern. Med.* 105:883–885.
23. May, G.R., L.R. Sutherland, and J.B. Meddings. 1993. Is small intestinal permeability really increased in relatives of patients with Crohn's disease? *Gastroenterology*. 104:1627–1632.
24. Wyatt, J., H. Vogelsang, W. Hubl, T. Waldhoer, and H. Lochs. 1993. Intestinal permeability and the prediction of relapse in Crohn's disease. *Lancet*. 341:1437–1439.
25. Schneeberger, E.E., and R.D. Lynch. 2004. The tight junction: a multifunctional complex. *Am. J. Physiol. Cell Physiol.* 286:C1213–C1228.

26. Gewirtz, A.T., Y. Liu, S.V. Sitaraman, and J.L. Madara. 2002. Intestinal epithelial pathobiology: past, present and future. *Best Pract. Res. Clin. Gastroenterol.* 16:851–867.
27. Clayburgh, D.R., L. Shen, and J.R. Turner. 2004. A porous defense: the leaky epithelial barrier in intestinal disease. *Lab. Invest.* 84:282–291.
28. Furuse, M., K. Furuse, H. Sasaki, and S. Tsukita. 2001. Conversion of zonulae occludentes from tight to leaky strand type by introducing claudin-2 into Madin-Darby canine kidney I cells. *J. Cell Biol.* 153: 263–272.
29. Turksen, K., and T.C. Troy. 2004. Barriers built on claudins. *J. Cell Sci.* 117:2435–2447.
30. Simonovic, I., J. Rosenberg, A. Koutsouris, and G. Hecht. 2000. Enteropathogenic Escherichia coli dephosphorylates and dissociates occludin from intestinal epithelial tight junctions. *Cell. Microbiol.* 2:305–315.
31. Ma, T.Y., G.K. Iwamoto, N.T. Hoa, V. Akotia, A. Pedram, M.A. Boivin, and H.M. Said. 2004. TNF-alpha-induced increase in intestinal epithelial tight junction permeability requires NF-kappa B activation. *Am. J. Physiol. Gastrointest. Liver Physiol.* 286:G367–G376.
32. Strober, W., I.J. Fuss, and R.S. Blumberg. 2002. The immunology of mucosal models of inflammation. *Annu. Rev. Immunol.* 20:495–549.
33. Crohn, B.B., L. Ginzburg, and G.D. Oppenheimer. 1932. Regional ileitis: a pathologic and clinical entity. 1932. *Mt. Sinai J. Med.* 99: 1323–1329.
34. Matsumoto, S., Y. Okabe, H. Setoyama, K. Takayama, J. Ohtsuka, H. Funahashi, A. Imaoka, Y. Okada, and Y. Umesaki. 1998. Inflammatory bowel disease-like enteritis and caecitis in a senescence accelerated mouse P1/Yit strain. *Gut.* 43:71–78.
35. Rivera-Nieves, J., G. Bamias, A. Vidrich, M. Marini, T.T. Pizarro, M.J. McDuffie, C.A. Moskaluk, S.M. Cohn, and F. Cominelli. 2003. Emergence of perianal fistulizing disease in the SAMP1/YitFc mouse, a spontaneous model of chronic ileitis. *Gastroenterology.* 124: 972–982.
36. Kosiewicz, M.M., C.C. Nast, A. Krishnan, J. Rivera-Nieves, C.A. Moskaluk, S. Matsumoto, K. Kozaiwa, and F. Cominelli. 2001. Th1-type responses mediate spontaneous ileitis in a novel murine model of Crohn's disease. *J. Clin. Invest.* 107:695–702.
37. Takedatsu, H., K. Mitsuyama, S. Matsumoto, K. Handa, A. Suzuki, H. Takedatsu, H. Funabashi, Y. Okabe, T. Hara, A. Toyonaga, and M. Sata. 2004. Interleukin-5 participates in the pathogenesis of ileitis in SAMP1/Yit mice. *Eur. J. Immunol.* 34:1561–1569.
38. Olson, T.S., G. Bamias, M. Naganuma, J. Rivera-Nieves, T.L. Burcin, W. Ross, M.A. Morris, T.T. Pizarro, P.B. Ernst, F. Cominelli, and K. Ley. 2004. Expanded B cell population blocks regulatory T cells and exacerbates ileitis in a murine model of Crohn disease. *J. Clin. Invest.* 114:389–398.
39. Marini, M., G. Bamias, J. Rivera-Nieves, C.A. Moskaluk, S.B. Hoang, W.G. Ross, T.T. Pizarro, and F. Cominelli. 2003. TNF-alpha neutralization ameliorates the severity of murine Crohn's-like ileitis by abrogation of intestinal epithelial cell apoptosis. *Proc. Natl. Acad. Sci. USA.* 100:8366–8371.
40. Bamias, G., M. Marini, C.A. Moskaluk, M. Odashima, W.G. Ross, J. Rivera-Nieves, and F. Cominelli. 2002. Down-regulation of intestinal lymphocyte activation and Th1 cytokine production by antibiotic therapy in a murine model of Crohn's disease. *J. Immunol.* 169:5308–5314.
41. Kozaiwa, K., K. Sugawara, M.F. Smith Jr., V. Carl, V. Yamschikov, B. Belyea, S.B. McEwen, C.A. Moskaluk, T.T. Pizarro, F. Cominelli, and M. McDuffie. 2003. Identification of a quantitative trait locus for ileitis in a spontaneous mouse model of Crohn's disease: SAMP1/YitFc. *Gastroenterology.* 125:477–490.
42. Sugawara, K., T.S. Olson, C.A. Moskaluk, B.K. Stevens, S. Hoang, K. Kozaiwa, F. Cominelli, K.F. Ley, and M. McDuffie. 2005. Linkage to peroxisome proliferator-activated receptor-gamma in SAMP1/YitFc mice and in human Crohn's disease. *Gastroenterology.* 128:351–360.
43. Burns, R.C., J. Rivera-Nieves, C.A. Moskaluk, S. Matsumoto, F. Cominelli, and K. Ley. 2001. Antibody blockade of ICAM-1 and VCAM-1 ameliorates inflammation in the SAMP-1/Yit adoptive transfer model of Crohn's disease in mice. *Gastroenterology.* 121:1428–1436.
44. El Asmar, R., P. Panigrahi, P. Bamford, I. Berti, T. Not, G.V. Coppa, C. Catassi, and A. Fasano. 2002. Host-dependent zonulin secretion causes the impairment of the small intestine barrier function after bacterial exposure. *Gastroenterology.* 123:1607–1615.
45. Meddings, J.B., and I. Gibbons. 1998. Discrimination of site-specific alterations in gastrointestinal permeability in the rat. *Gastroenterology.* 114:83–92.
46. Korngold, B., and J. Sprent. 1978. Lethal graft-versus-host disease after bone marrow transplantation across minor histocompatibility barriers in mice. Prevention by removing mature T cells from marrow. *J. Exp. Med.* 148:1687–1698.
47. Neutra, M.R., N.J. Mantis, and J.P. Kraehenbuhl. 2001. Collaboration of epithelial cells with organized mucosal lymphoid tissues. *Nat. Immunol.* 2:1004–1009.
48. Bruewer, M., A. Luegering, T. Kucharzik, C.A. Parkos, J.L. Madara, A.M. Hopkins, and A. Nusrat. 2003. Proinflammatory cytokines disrupt epithelial barrier function by apoptosis-independent mechanisms. *J. Immunol.* 171:6164–6172.
49. Madsen, K.L., D. Malfair, D. Gray, J.S. Doyle, L.D. Jewell, and R.N. Fedorak. 1999. Interleukin-10 gene-deficient mice develop a primary intestinal permeability defect in response to enteric microflora. *Inflamm. Bowel Dis.* 5:262–270.
50. Dvorak, A.M., and G.R. Dickersin. 1980. Crohn's disease: transmission electron microscopic studies. I. Barrier function. Possible changes related to alterations of cell coat, mucous coat, epithelial cells, and Paneth cells. *Hum. Pathol.* 11:561–571.
51. Scott, K.G., J.B. Meddings, D.R. Kirk, S.P. Lees-Miller, and A.G. Buret. 2002. Intestinal infection with Giardia spp. reduces epithelial barrier function in a myosin light chain kinase-dependent fashion. *Gastroenterology.* 123:1179–1190.
52. Kucharzik, T., S.V. Walsh, J. Chen, C.A. Parkos, and A. Nusrat. 2001. Neutrophil transmigration in inflammatory bowel disease is associated with differential expression of epithelial intercellular junction proteins. *Am. J. Pathol.* 159:2001–2009.
53. Bradley, P.P., D.A. Priebat, R.D. Christensen, and G. Rothstein. 1982. Measurement of cutaneous inflammation: estimation of neutrophil content with an enzyme marker. *J. Invest. Dermatol.* 78:206–209.
54. Boughton-Smith, N.K.,J.L. Wallace, and B.J. Whittle. 1988. Relationship between arachidonic acid metabolism, myeloperoxidase activity and leukocyte infiltration in a rat model of inflammatory bowel disease. *Agents Actions.* 25:115–123.